Proceedings of the 15th International Symposium on the
Packaging and Transportation of Radioactive Materials
PATRAM 2007
October 21-26, 2007, Miami, Florida, USA

SIMULATIONS OF NATURAL CONVECTION/RADIATION HEAT TRANSFER FOR HORIZONTAL AND VERTICAL ARRAYS OF HEATED RODS INSIDE A UNIFORM TEMPERATURE ENCLOSURE

N. R. Chalasani
Research Assistant
Mechanical Engineering Department
University of Nevada, Reno
Email: chalasan@unr.nevada.edu

Pablo E. Araya
Research Assistant
Mechanical Engineering Department
University of Nevada, Reno
Email: arayap@unr.nevada.edu

Miles Greiner
Professor of Mechanical Engineering
Mechanical Engineering Department
University of Nevada, Reno
Email: greiner@unr.edu

ABSTRACT

In the current work, numerical simulations and experiments of an 8×8 square array of heater rods within an aluminum enclosure have been performed. This geometry represents the region inside the channel of a boiling water reactor (BWR) fuel assembly between two consecutive spacer plates. The simulation model and the experimental apparatus can be oriented horizontally or vertically, to represent transport or storage configurations. The interior void is filled with air at ambient pressure conditions. All rods dissipate at the same heating rate. In the experiment, this is controlled using a variable power supply. The temperatures are measured in the experiment by thermocouples that are placed within the enclosure walls, on the endplates, and in 31 of the 64 heater rods at their axial mid-planes. The three-dimensional computational fluid dynamics (CFD) model is based on the dimensions of experimental apparatus. Natural convection/radiation simulations are performed using the Fluent package at the same average wall temperatures and rates of heat generation measured from the experiment. Simulation results of rod temperatures are compared to experimental results to assess the accuracy of the three-dimensional computational fluid dynamics (CFD) simulations. Simulation results show good agreement with measured temperatures. Average simulated rod temperatures are lower than measured data by up to 1.2% in horizontal orientation and higher than measured by up to 1.3% in vertical orientation.

INTRODUCTION

The goal of this work is to perform an experiment that benchmarks a CFD software code. The code calculates radiation and natural convection across gaps and conduction in the solid regions of an enclosed heated square rod array. The experiment is based on the geometry of a

boiling water reactor (BWR) assembly and is designed to improve understanding of the heat transfer during dry storage and transport. Experimental measurements are compared to CFD simulation results in order to gain confidence in the code.

Spent nuclear fuel is placed in thick-walled casks for dry storage or transport [1, 2]. Individual assemblies are placed in the containment region at the center of the cask where they are supported within square cross section openings of a basket structure. A truck transport cask can contain 4 assemblies [2] and a rail cask 21 assemblies [1]. The containment region of the casks is evacuated and backfilled with a non-oxidizing cover gas.

Each assembly is composed of a square array of heat-generating fuel rods that can vary from 7×7 to 9×9 for BWR and from 14×14 to 18×18 for pressurized water reactor (PWR) assemblies [3, 4]. The fuel rods are made of UO_2 pellets housed in a zircaloy cladding tube. The pellets continue to generate heat after being removed from reactor operation. The amount of heat generated depends on the reactor burn-up and the post-reactor pool cooling time. However, the rod cladding temperature must not exceed its integrity temperature limit of 400°C during normal transport [5]. This can limit the number and heat generation rate of the fuel assemblies that can be transported in a package. BWR assemblies may or may not include an outer shielding channel when placed within a cask. Both BWR and PWR may have non-heated guide tubes or instrument tubes within the array.

Finite element thermal models of casks have been used to predict the cladding temperature for different fuel heat generation rates. In the past, computational resources did not allow the use of models that accurately represented the fuel geometry. Fuel regions were replaced by solids with simplified effective thermal conductivities (ETC) [2].

Manteufel and Todreas [6] developed an ETC based on one-dimensional conduction and radiation within a rectangular array of heated fuel rods immersed in stagnant gas. However, this model neglects effects of two-dimensional heat transfer at the corners, and the unheated components such as instrument tubes, guide tubes, and external channels.

Another ETC model was developed by Bahney and Lotz [4]. This model is based on results from two-dimensional finite element simulations of conduction and radiation heat transfer within fuel assembly/cover gas regions inside uniform temperature baskets. Several BWR and PWR fuel assemblies were accurately represented, including unheated components. The maximum cladding temperatures were determined at various assembly heat generation rates and basket wall temperatures. Simulation results were used to develop an ETC model. However, the results were not compared to experimental data and mesh independence was not explicitly demonstrated.

Greiner et. al [7] used different ETCs to determine the peak cladding temperature (T_{PC}) versus fuel heat load (Q) of a rail cask containing 21 PWR assemblies, under normal hot day conditions. They also determined the cask thermal dissipation capacity (Q_{TDC}) which is the total heat load that elevates the cladding to the temperature integrity limit. Their simulations showed that the predicted T_{PC} varied significantly for different ETCs. Moreover, when the fuel heat generation rate is near its Q_{TDC}, the temperature of the center fuel basket is nearly isothermal at ~380ºC. However, near the package edge, the average basket temperature is ~350ºC and non-uniform, varying by ~60ºC [7].

One shortcoming of using ETC models to simulate heat transfer within fuel assembly/cover gas regions is that these models approximate heat flux at a location based on the temperature and spatial gradient at that location. This is not universally appropriate when natural convection and/or thermal radiation effects are significant. For example, natural convection heat transfer is affected by the local fluid velocity, which depends on temperatures at other locations. In addition, the radiant heat flux at a location is affected by temperatures at a distance from that location. As a result, it is not currently known if ETC models that are accurate in basket

openings near the cask center in which the wall temperature is essentially uniform can be used to accurately model heat transfer in periphery cells with non-uniform temperature profiles [7].

Current resources allow for the use of computational meshes that accurately model the fuel geometry. The Q_{TDC} from CFD simulations of a truck cask [8] and a rail cask [9] have been compared to predictions from ETCs. These studies calculate the T_{PC} within the casks. Package temperatures were presented for a range of fuel heat generation rates, Q. The CFD simulations consistently predict lower T_{PC} and larger Q_{TDC} for a given Q than ETC models. However, CFD must be benchmarked experimentally under relevant conditions before it can be used with confidence to predict Q_{TDC}.

Experiments were performed in full vertical storage casks where the fuel was replaced with oversized heating elements [10]. Although temperature data was obtained for cask elements such as the basket and liners, the amount of data taken from the entire shipping cask was sparse and the boundary conditions and geometry of the experiment were not well documented. Therefore, there is insufficient information to characterize individual fuel assemblies and benchmark models or CFD simulations.

Experiments have been performed for a horizontal 8×8 BWR mock-up [11] and for a vertical material retrievable storage (MRS) cask [12]. However, in both cases, there is insufficient information available from the experiments to accurately model them with CFD. Also, the boundary conditions and/or geometry of the experiments were not appropriate for conditions where the cask is near its thermal dissipation capacity. In addition, Canaan and Klein [13] constructed an 8×8 experiment to obtain temperature data that was later compared to numerical simulations [14]. However, their wall boundary temperatures were much cooler than those expected in a cask basket cell.

Simulations based on the experiment of Lovett and Arya and Keyhani have been performed [15, 16]. These were intended to gain experience in using and benchmarking the CFD code. These simulations consistently reproduce the measurements; however, new experiments are needed that are closer to the conditions within a cask that is near its thermal dissipation capacity.

In the current work CFD-based calculations are benchmarked against relevant experimental data for a range of conditions. The experiment is a mock-up of an 8×8 BWR assembly. Heater rods are used to represent the fuel rods and an aluminum enclosure is built to house the rod array and represent an isothermal BWR channel. Wall and rod temperatures are obtained for a range of rod heat generation rates. Temperature data from the experiment is then compared to three-dimensional CFD temperature predictions. This work allows the assessment of the computational methods. Future work will include running the benchmark experiment at different pressures, with different cover gases and non-uniform wall temperatures.

EXPERIMENTAL FACILITY

Figure 1(a) shows the 8×8 heater rod array that was assembled for the experimental facility. The experimental setup is 10% smaller than an actual BWR assembly. It considers the region between two grid spacers and within the channel.

There are sixty-four Watlow tubular heater rods, each 1.1 cm in diameter and 67.3 cm in length. The heaters are arranged in a square pattern with center-to-center pitch spacing of 1.45 cm. Each rod contains an electric resistance heater coil with power leads on both ends. Rods are connected to a power supply that can be run at a generation of up to 1000 W. The rods are made of a compressed MgO core that is surrounded by an Incoloy tube sheath. Fig. 1(b) shows the internal NiCr coil that generates heat. This leaves a 3.2 cm (1.25 inch) unheated section on both ends of the rod. Thirty-one rods have a type-K thermocouple at the mid-plane with leads exiting from both ends. The side and section views of the heater rods in Figs. 1(b) and 1(c) show the

approximate position of the internal thermocouple. The exact radial position of the coil and TC junction are not specified by the manufacturer.


(a)

(b)

(c)
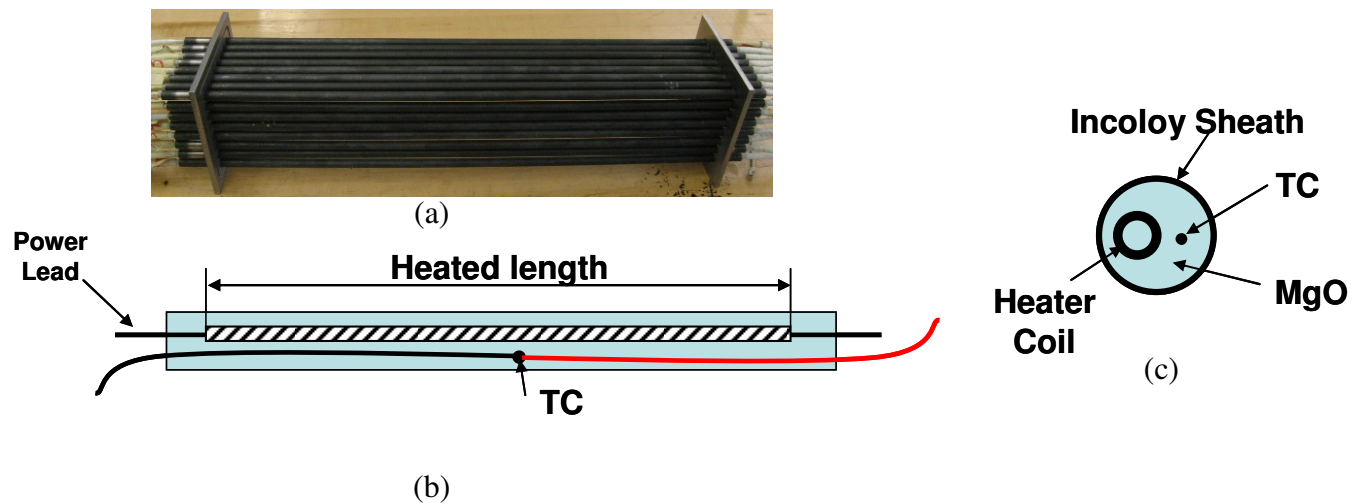
Figure 1 Experimental facility. (a) 8×8 heater rod array, (b) heater rod side view, and (c) heater rod section.

Figure 2(a) shows the aluminum enclosure. The enclosure is a square section tube of 11.8 cm inner width with a 2.54 cm thick wall. Two square stainless steel endplates are bolted on each end of the aluminum enclosure. Sixty-four holes are drilled into the four endplates to hold the rods in place. To provide a tight seal between the endplates and enclosure O-rings (not shown) made of silicon rubber are placed in a groove that is cut into each endplate. They are sandwiched between the endplates and aluminum enclosure ends. K-type thermocouples are used for the measurement of wall surface temperature. They consist of 21 TC probes on the enclosure wall seen in Fig. 2(a) and 4 surface TCs on each endplate shown in Fig. 2(b). Five blind holes of 2.29 cm depth are made on each aluminum wall for the TC probes. Four of the five blind holes are located at 2.54 cm away at the center of the nearest edge. The leftover thermocouple is at the center of the wall. The center probe located on the top surface, is used as a reference common TC. An additional TC located near the reference common TC measures the absolute temperature of the common point. It has independent leads that are connected to an ice point reference signal conditioner (Omega DRF-TC). The ambient temperature is also monitored independently.

Only the interior channel region of a BWR is considered in this mock-up. Araya and Greiner [17] performed two-dimensional CFD simulations of natural convection and radiation heat transfer within a uniform temperature basket cell. They showed that the channel surrounding the fuel rods and the gap between the channel and outer basket can be modeled analytically. This reduces the complexity of the geometry to be studied.

All TCs used are connected in series to the reference common TC. The voltage from each TC pair is measured using a data acquisition board (National Instruments NI-6225) inside a standard computer work station. The voltage is a function of the difference between the TC junction and the reference junction (Ref-J). This setup allows for the input of up to 80 non-referenced, single-ended signals.
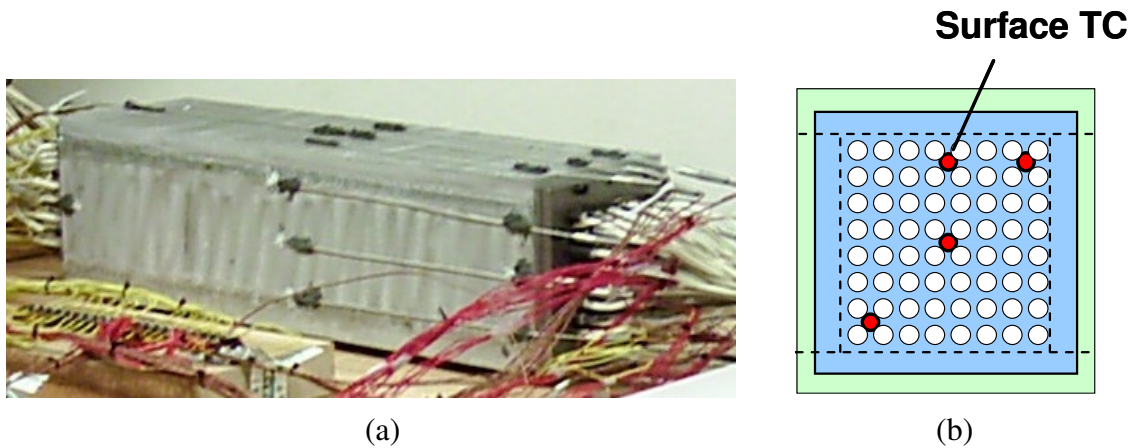
Figure 2 Experimental facility (a) enclosure with wall thermocouples, (b) endplate with locations of 4 surface TCs.

Experiments are run by setting the regulated DC power supply to deliver a total of 100, 200, or 300 Watts to the rod array. The LabVIEW software is used on the workstation to monitor and record individual thermocouple temperatures as well as ambient temperatures. After each power is set, all thermocouple voltages are sampled at a rate of 3000 samples/sec and averaged for 60 seconds to reduce the effects of radio frequency noise. The signals are monitored until a steady state is reached. Then the steady state regime is monitored for an extended time and the temperature data is averaged in time for each channel. The resulting average values are representative of the steady state TC temperatures.

Figure 3 shows the time evolution of the horizontal experiment for a heat load of 200 Watts. Included in the figure are rod temperatures, wall and endplate temperatures, the reference common temperature (Ref-J), and the ambient temperature (T_{AMB}). Initially, all temperatures increase until a steady state is reached at approximately 10 hours. Then, to acquire temperature data, the experiment is continued at a steady state. After approximately 12 hours, the temperatures began to increase again due to an increase in ambient temperature; this trend continues until a new steady state is reached. However, the rise in temperature during this transition is only 2°C. The total run of the experiment is 22 hours. This data is time averaged for the last 10 hours to reduce noise on individual thermocouple data. The maximum noise found at 300 Watts, with a 3 kHz sampling rate, is ±0.7 °C for horizontal orientations and ±0.8°C for vertical orientations. Similar or lower noise is observed for all heat loads in both vertical and horizontal experiments. Once time-average data is obtained for each wall TC, the five TC temperatures for each aluminum wall are averaged to obtain an average wall temperature. The same procedure is followed for the four thermocouples on each endplate to obtain average endplate temperatures. These average temperatures are later used as temperature boundary conditions in the CFD simulation model.

Measured Wall Temperatures

Figure 4(a) shows average temperatures for both the end-plates and aluminum walls when the apparatus is horizontal as a function of heat generation rate Q. At 200 W, the aluminum walls are isothermal to within ±2.5ºC and the endplates are 5ºC hotter than the aluminum walls (due to contact with heater rods). Both, the endplates and aluminum walls have nearly equal average temperatures. Figure 4(b) shows average temperatures for both endplates and aluminum walls when the apparatus is vertical. The upper endplate is 3.5ºC hotter than the

5

lower one due to buoyancy-induced gas motion inside and outside the enclosure whereas the sidewalls are isothermal within ±0.5ºC. These average wall temperatures are used as boundary conditions in the CFD simulations.
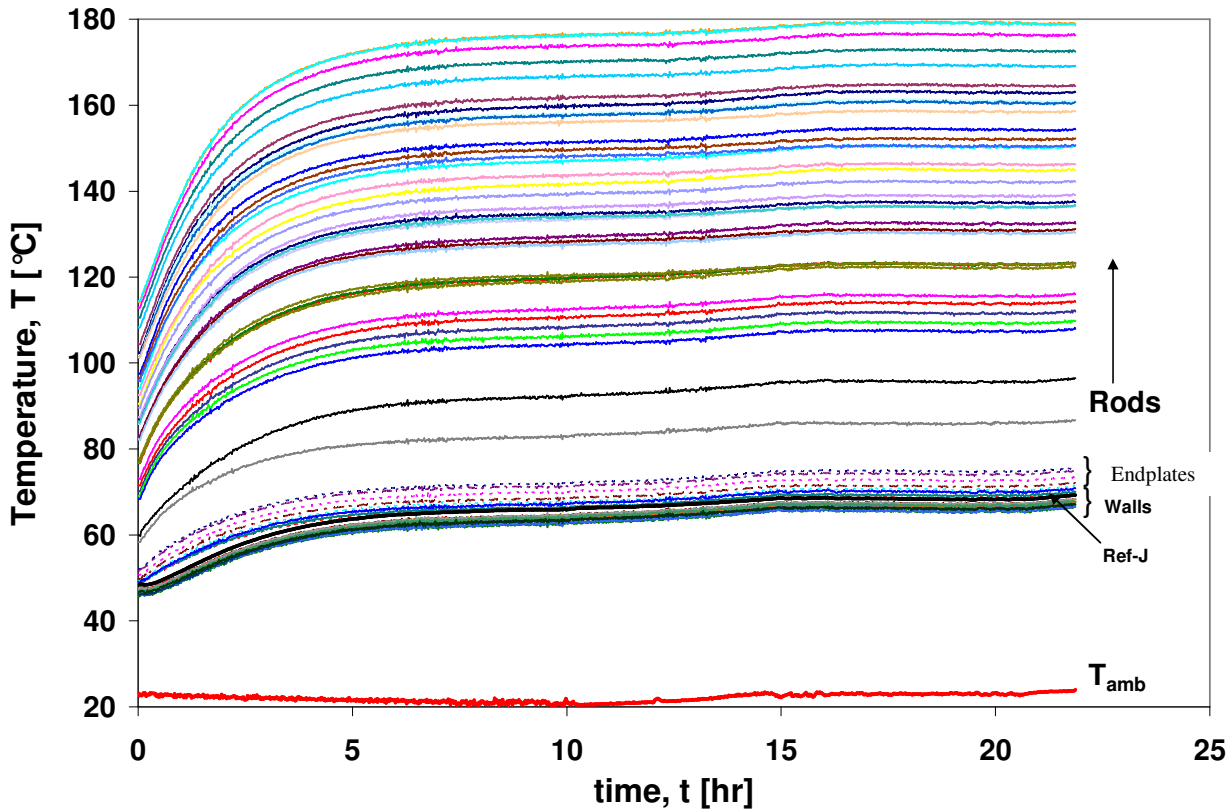

Figure 3 Time evolution of thermocouple readings for the experiment placed horizontally and run at 200 W.
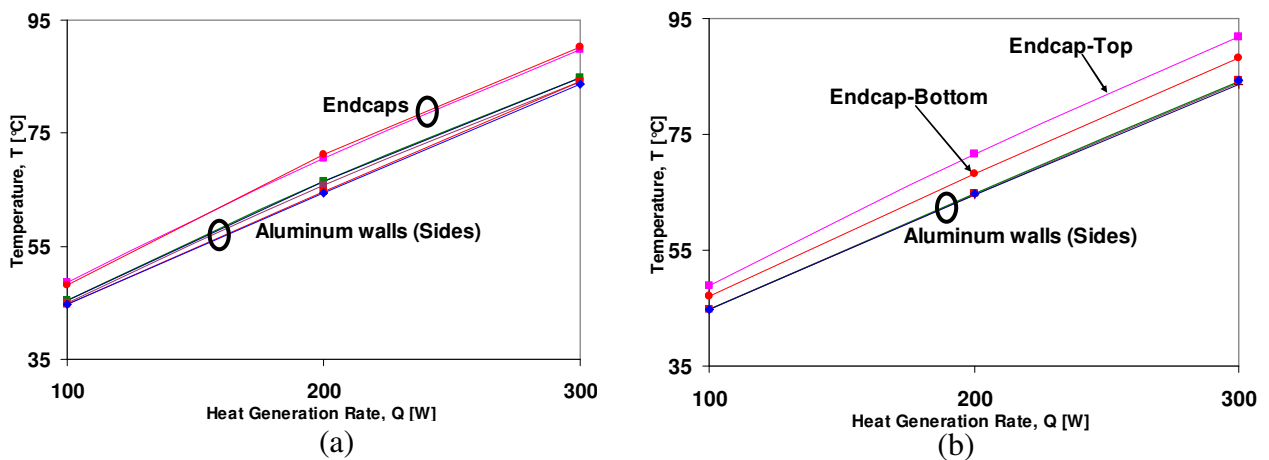

Figure 4 Measured rod and wall temperatures for (a) Horizontal and (b) Vertical.
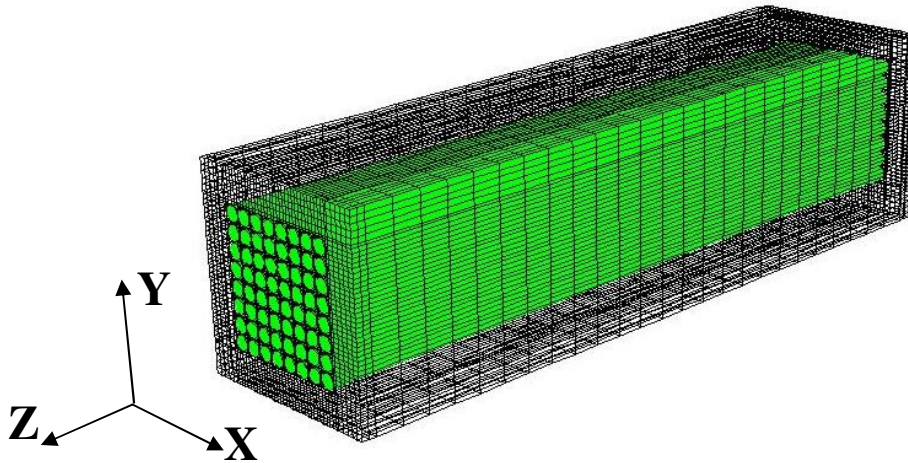
NUMERICAL MODEL

Figure 5 shows the three-dimensional (3D) finite-volume mesh used to simulate conduction, natural convection and radiation heat transfer in the heater array experiment. The mesh is composed of 175k elements. An x-y plane grid was first created and then extruded in the z direction to create this 3D mesh in Patran/thermal.

6

The dimensions and materials of the experimental facility were used to construct the simulation model. Both the rods and the enclosure materials are solids. The section of the heater rod is modeled such that the heat-generating NiCr coil is neglected and a uniform volumetric heat generation is applied throughout the MgO within the rod. The void region between the rods and the enclosure is filled with atmospheric pressure air.

The simulations presented in this study were run using the commercial FLUENT 6.3.26. FLUENT solves the conservation of mass, while energy equations are solved using a finite-volume method with discretized governing equations. Pressure-velocity coupling is solved for using the SIMPLE method. The mesh is constructed and the governing equations are solved with double precision. The steady solver and a second-order upwind scheme is used for solving the momentum and energy equations. The buoyancy-induced flow is generated by adding the gravitational force $g_{Horizontal} = g_{Vertical} = 9.8$ m/s^2 in the –y direction for horizontal orientation and the –z direction for vertical orientation. A temperature-dependent density of the cover gas is considered. Also, radiation is solved for gray diffuse surfaces using the discrete ordinates method. The values of surface emissivity are 0.8 for the heater rod (specified by manufacturer), 0.6 for the stainless steel endplates, and an estimated value of 0.5 for the aluminum walls [18].

As measured in the experiments, the average top, bottom, left, and right temperatures of the endplate and the enclosure are imposed as isothermal boundary conditions in the model. Results from the simulations are then compared to the rod TC temperatures obtained with the experimental facility.


Figure 5 Numerical model grid.

Results

Figure 6(a) and 6(b) show temperature contours on the heater surface from the CFD simulations at a heat load of 200 Watts for both horizontal and vertical orientations. The presence of natural convection is observed in a 1/2 slice contour by a displaced central hot region in +y direction for horizontal and +z direction for vertical orientations. The axial temperature gradient is stronger in the upper half of the vertical simulations than in the lower. The minimum temperature T_{MIN} is 7.7°C lower for vertical than for horizontal simulations, but the maximum rod temperature T_{MAX} is 0.6°C higher for vertical than for horizontal simulations.

Figure 7(a) and 7(b) show mid-plane temperature contours and velocity vectors from CFD simulations at 200 W for horizontal and vertical orientations. The buoyancy of the air causes upward-rising currents at the center of the domain and downward currents toward the walls. This causes the central hot region to be above center for both orientations.

Figure 8 shows the maximum speeds S_{MAX} obtained for both horizontal and vertical simulations at 100, 200 and 300 Watts. For vertical orientation at 200 W, the maximum upward speed is 21 cm/s and located above the center of the axial mid-plane. The maximum downward speed is 20 cm/s at the corners of the axial mid-plane. Vertical simulations always exhibit significantly higher speeds because it involves a much larger vertical dimension. Also, the relative increase of S_{MAX} with respect to heat load is lower at higher heat loads because of the increased presence of radiation heat transfer.
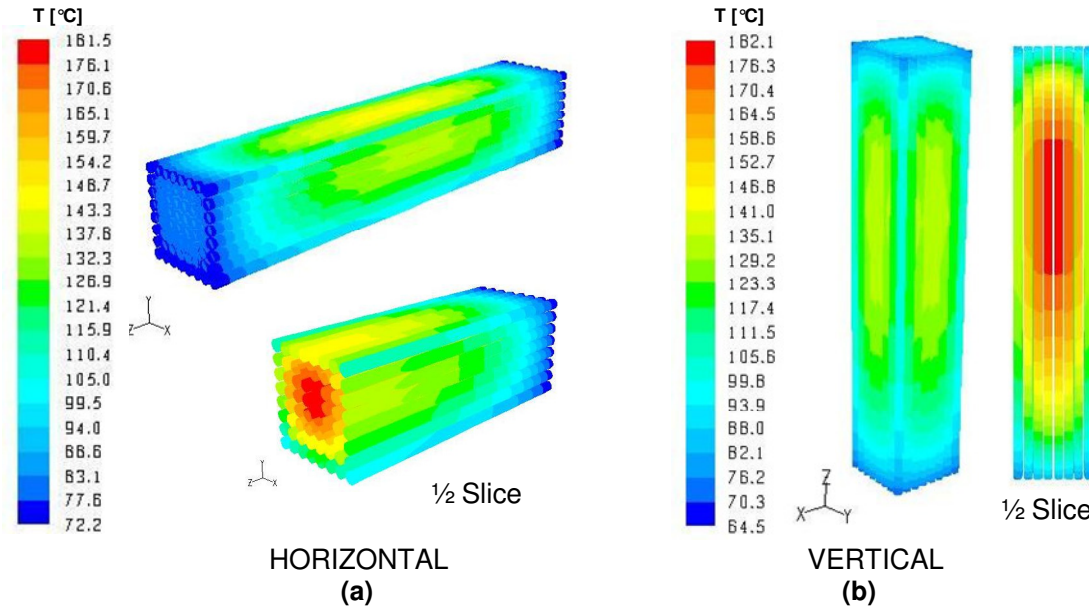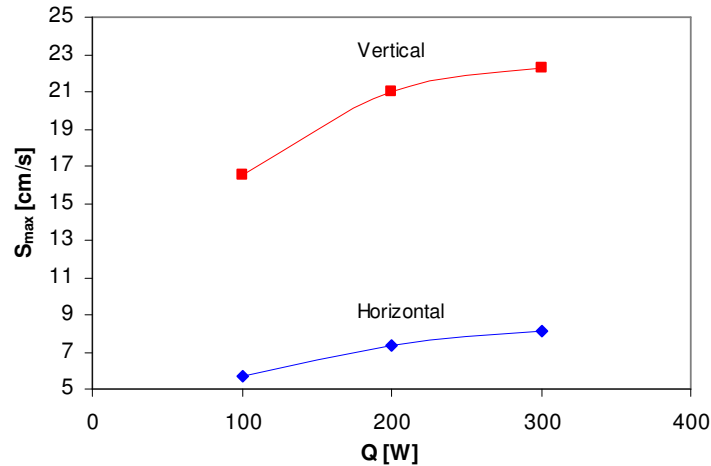

Figure 6 CFD Temperature Contours for 200 W (a) horizontal and (b) vertical simulations.
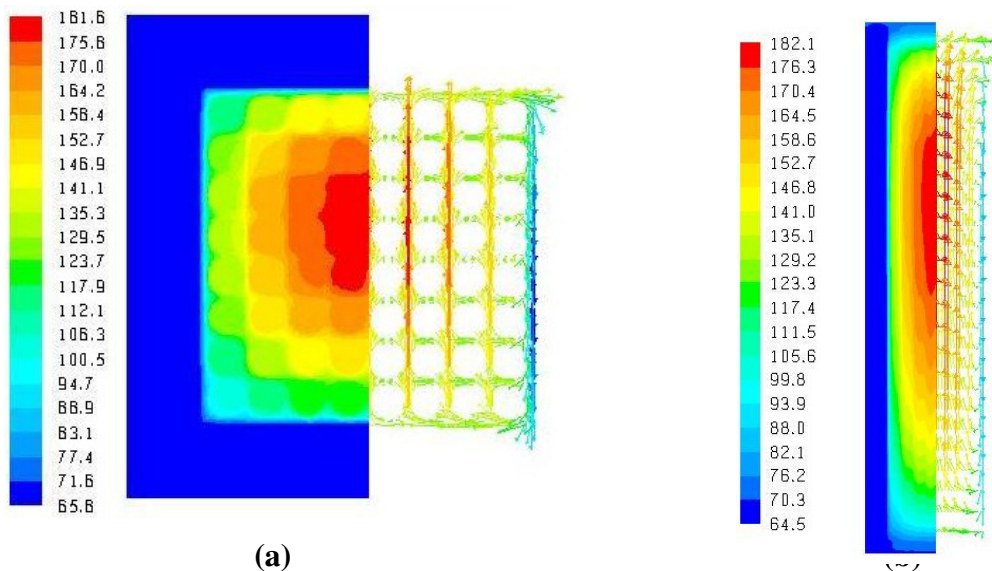
Figure 7 Temperature contours and velocity vectors for CFD results at 200 W (a) horizontal (cross-Section mid-plane) and (b) vertical (axial mid-plane).

Figure 8 Maximum Speed for the CFD as a function of heat load for both horizontal and vertical simulations.

Figure 9a is a cross section through the test apparatus showing the location of all 64 heater rods. The 31 rods with working thermocouples at their axial mid-plane are shown using solid circles. The four columns on the left side are labeled 1-4, and 1'-4' on the right. The four upper rows are labeled A-D, and the lower are labeled A'-D'. A gravity vector in the figure shows which rows are at the bottom when the apparatus is horizontal.

When the test section is in either the horizontal or vertical orientation, the symmetry of the geometry and boundary conditions indicates that the results from the left and right side will be nearly identical. Ten of the thermocouple locations on the left side have a corresponding thermocouple on the right side. Differences between corresponding pairs indicate a configuration error. This uncertainty is caused by uncontrolled differences in heater resistances, surface emissivities, thermocouple/heater placement within rods, and wall surface temperatures. When the apparatus is in the vertical orientation, symmetry again suggest that the temperatures from rows A-D will be nearly identical to those in rows A'-D'.

Figure 9b shows the measured and simulated temperature difference versus distance from the bottom aluminum wall. These results are for the horizontal orientation for a heat generation rate of 200 W. This difference is the temperature at a location minus the lowest temperature on the aluminum walls. Simulated results are shown along lines that pass through the centers of the rods in columns 1-4 and columns 1'-4'. The simulated results from Columns 1-4 and 1'-4' are sufficiently close that only four lines are visible. Measured temperatures are shown using symbols. Error bars are used for locations where pairs of temperatures on the left and right side of the apparatus are measured. In those cases, the symbol represents the average of the two measurements, and the error bars show one standard deviation on either side.

General symmetry is observed in the measured data, though a difference of 20°C is seen in the top-center thermocouple pair (4A-4'A) and a difference of 9°C in the bottom-center pair (4A'-4'A'). The remaining thermocouple pairs show differences ranging from 0.2°C to 6°C and the data are not skewed to one particular side. The simulation profiles exhibit the same trends as the measured data. The maximum measured temperature difference between a heater and the wall is 113.4°C in column 4 and row C (4C). The simulated temperature difference is 1.2% larger than the measured data.

Figure 10(a) shows the measured and simulated temperature difference versus heat generation rate for heater rod 4C when the orientation of the apparatus is horizontal and vertical. This difference is the temperature of the heater rod 4C minus lowest temperature on the aluminum walls. Simulated temperature differences are shows using a line whereas the measured

data are shown using symbols. The difference between the simulated and measured data decreases as the heat generation rate decreases. At 300 W the temperature difference for rod 4C is 8.2°C higher when the apparatus is in the horizontal orientation than when it is vertical. Simulation accurately predicts trends with heat generation rate and orientation.

Figure 10 (b) shows the measured and simulated average temperature difference versus heat generation rate when the orientation of the apparatus is horizontal vertical. This difference is the average temperature of all the heater rods that contained thermocouples minus the lowest temperature on the aluminum walls. Simulated temperature differences are shown using lines whereas the measured data are shown using symbols. For Q ≤ 200 W, the measured average temperature is nearly the same in both vertical and horizontal orientations. At 300 W the average temperature is 1.8°C hotter when the apparatus is vertical. Simulations under-predicts ΔT_{AVG} by no more than 0.9 °C (1.2%) in horizontal and over-predicts by no more than 1.3°C (3%) in vertical. ΔT_{AVG} is generally higher for the vertical orientation by up to 2.3°C (2.3%) in CFD and by 1.8°C (1.9%) in experiments. Simulation accurately predicts trends with heat generation rate and orientation.
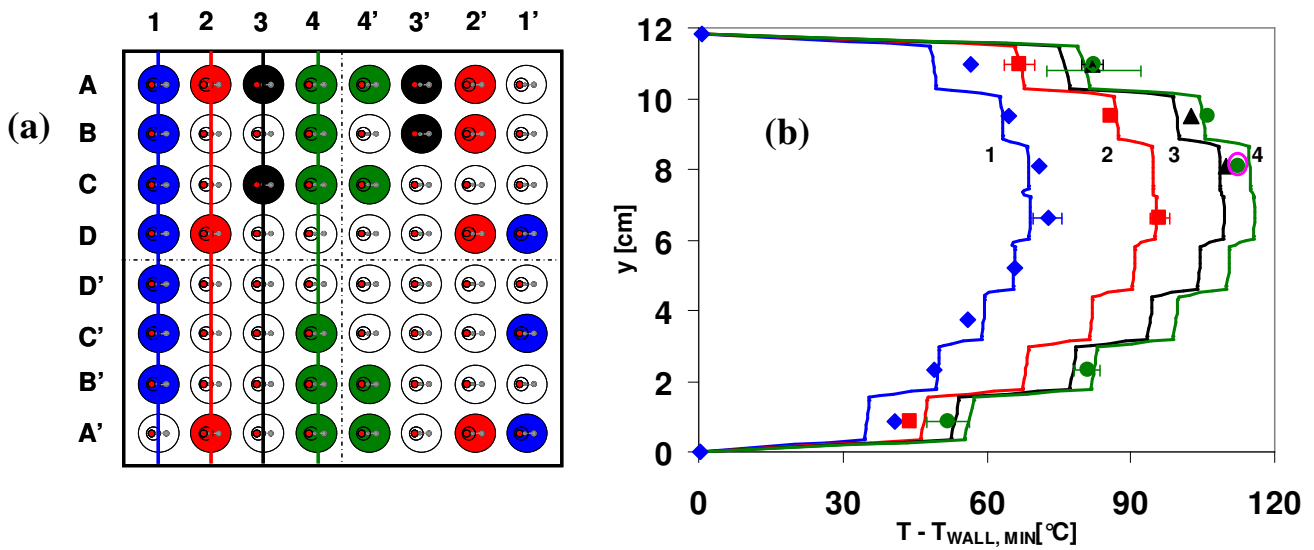

Figure 9 (a) Cross section through the test apparatus showing the location of the heater rods that contain thermocouple (b) measured and simulated temperature difference versus distanced from the interior surface of the aluminum wall.
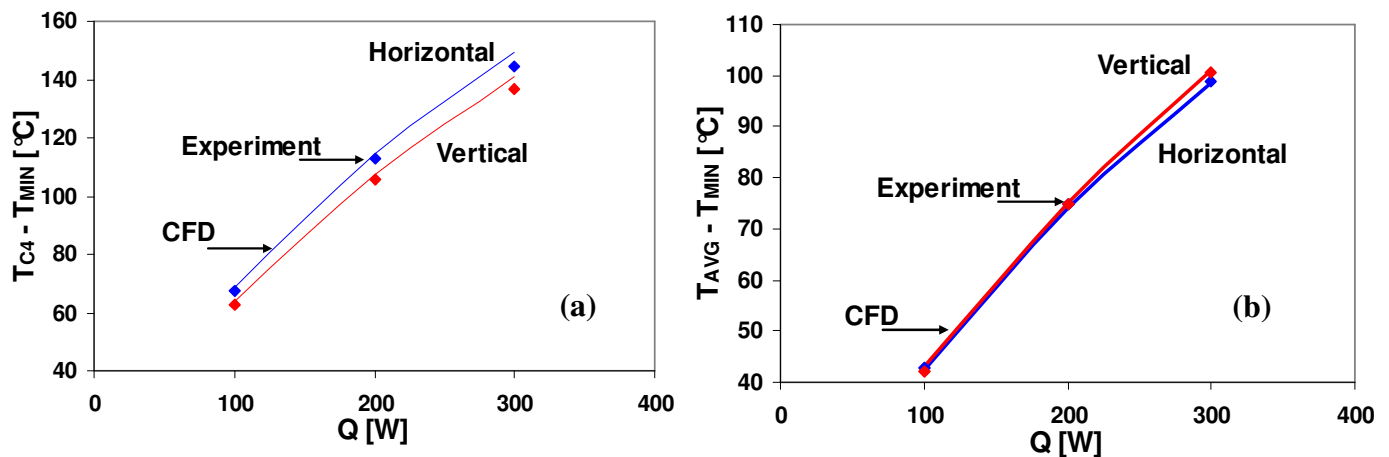

Figure 10 Temperature difference as a function of heat generation for both experiments and simulations (a) maximum temperature for rod (4C) (b) average temperature.

CONCLUSIONS

In the current work, numerical simulations and experiments using an 8×8 square array of heater rods within an aluminum enclosure have been performed. Both horizontal and vertical analyses are performed to study transport or storage configurations. The temperatures are measured in the experiment using thermocouples, placed within the enclosure walls, on the endplates, and in 31 of the 64 heater rods. Natural convection/radiation simulations are performed using a 3D CFD model in the Fluent package at the same rates of heat generation and average wall temperatures measured from the experiment. Experimental results show configuration (symmetry) and measurement uncertainties of 8.5°C and 0.7°C respectively. Simulation results of rod temperatures are compared to measured experimental data and are in good agreement. Both CFD and measured data show that natural convection is present. Temperature distributions as well as general trends with respect to varying heat load show good agreement between measured data and CFD results. In comparing CFD results to measured data, the average temperatures exhibit a maximum difference of 1.2% in horizontal orientation and 3% in vertical orientation.

NOMENCLATURE

BWR	Boiling Water Reactor
CFD	Computational Fluid Dynamics
DAQ	Data Acquisition Card
ETC	Effective Thermal Conductivity models
PWR	Pressurized Water Reactor
Q	Total heat load [W]
Q_{TDC}	Cask Thermal Dissipation Capacity
Ref-J	Temperature of reference junction [°C]
S	Flow speed (Velocity Magnitude) [cm/s]
S_{MAX}	Maximum flow speed [cm/s]
T	Local temperature [°C]
T_{AMB}	Ambient temperature [°C]
T_{AVGM}	Average rod temperature of instrumented rods [°C]
TC	Thermocouple
T_{MAX}	Maximum temperature [°C]
T_{MIN}	Minimum average wall temperature [°C]
T_{PC}	Peak Cladding Temperature

ACKNOWLEDGMENTS

REFERENCES

[1] U.S. Dept. of Energy, Office of Civilian Radioactive Waste Management (OCRWM), 1993, *Multi-Purpose Canister (MPC) Implementation Program Conceptual Design Phase Report*, DOE ID: A20000000-00811-5705-00002, Final Draft, Sept. 30,

[2] Meyer, R., and Grenier, R., 1994, *GA-4 Legal Weight Truck From-Reactor Spent Fuel Shipping Cask. Safety Analysis Report for Packaging (SARP).* Prepared by General Atomics for the Office of Civilian Radioactive Waste Management of the U.S. DOE.

[3] U.S. Dept. of Energy, Office of Civilian Radioactive Waste Management (OCRWM), 1987, *Characteristics of Spent Nuclear Fuel, High-Level Waste, and Other Radioactive Wastes Which May Require Long-Term Isolation*, DOE/RW-0184, December.

[4] Bahney, R.H., and Lotz, T.L., 1996, *Spent Nuclear Fuel Effective Thermal Conductivity Report*, U.S. DOE, Yucca Mountain Site Characterization Project Office, D.I.: BBA000000-01717-5705-00010 REV 00.

[5] Nuclear Regulatory Commission (NRC), 2005, *Cladding Considerations for the Transportation and Storage of Spent Fuel*, Interim Staff Guidance Report for the Spent Fuel Project Office of the U.S. NRC, ISG-11 R3; available at www.nrc.gov

[6] Manteufel, R.D., and Todreas, N.E., 1994, "Effective Thermal Conductivity and Edge Conductance Model for a Spent-Fuel Assembly", *Nuclear Technology*, Vol. 105, March, pp. 421-440

[7] Greiner, M., Gangadharan, K., and Gudipati, M., 2007, "Use of Fuel/Backfill Gas Effective Thermal Conductivity Models to Predict Basket and Fuel Cladding Temperatures within a Rail Package during Normal Transport," paper accepted for publication in *Nuclear Technology*. Volume 161, issue 3, December.

[8] Venigalla, V.V.R., and Greiner, M., 2007, "CFD Simulations of Natural Convection/Radiation Heat Transfer within the Fuel Regions of a Truck Cask for Normal Transport," PVP2007-26242, *Proceedings of the 2007 ASME Pressure Vessels and Piping Division Conference*, July 22-26, San Antonio, Texas.

[9] Gudipati, M., and Greiner, M., 2007, "CFD Simulations of Fuel Cladding and Basket Surface Temperatures in an MPC Rail Cask during Normal Transport," Proceedings of the 15th International Symposium on the Packaging and Transportation of Radioactive Materials (PATRAM).

[10] Unterzuber, R., Milnes, R.D., Marinkovich, B. A., and Kubancsek, G.M., 1982, *Spent-Fuel Dry-Storage Testing at E-MAD (March 1978 through March 1982.)* Prepared for the US DOE Commercial Spent Fuel Management Program Office at the Pacific Northwest Laboratory, B-D3339-A-G. September.

[11] Lovett, P.M., 1991, *An Experiment to Simulate the Heat Transfer Properties of a Dry, Horizontal Spent Nuclear Fuel Assembly.* M.S. Thesis, Nuclear Eng., Massachusetts Institute of Technology.

[12] Arya, M.S., and Keyhani, M., 1990, *Convective Heat Transfer in a Sealed Vertical Storage Cask Containing Spent-Fuel Canisters*. M.S Thesis, Mechanical Eng., University of Tennessee, Knoxville.

[13] Canaan, R.E., and Klein, D.E., 1996, "An Experimental Investigation of Natural Convection Heat Transfer within Horizontal Spent-Fuel Assemblies," *Nuclear Technology*, December, Vol.116, pp. 306-318.

[14] Canaan, R E., and Klein, D.E., 1998, "A Numerical Investigation of Natural Convection Heat Transfer within Horizontal Spent-Fuel Assemblies", *Nuclear Technology*, Vol. 123, Aug. pp. 193-208.

[15] Araya, P.E., and Greiner, M. 2006, "Benchmark Natural Convection/Radiation Simulations within an Enclosed Array of Horizontal Heated Rods", PVP2006-ICPVT11-94021, *Proceedings of PVP 2006 ASME Pressure Vessels and Piping Division Conference,* July 23-27, Vancouver, BC.

[16] Chalasani, N.R., and Greiner, M. 2006, "Natural Convection/Radiation Heat Transfer Simulations of an Enclosed Array of Vertical Rods", PVP2006-ICPVT11-93734, *Proceedings of PVP 2006 ASME Pressure Vessels and Piping Division Conference,* July 23-27, Vancouver, BC.

[17] Araya, P.E., and Greiner, M. "Use of Regular rod Arrays to Model Heat transfer From BWR Fuel Assemblies Inside Transport Casks, PVP2007-26686, *Proceedings of the 2007 ASME Pressure Vessels and Piping Division Conference*, July 22-26, San Antonio, Texas.

[18] Modest, M.F., 2003, *Radiative Heat Transfer*, 2nd Edition, Academic Press, San Diego, CA.